34th Annual International Conference of the IEEE EMBS
San Diego, California USA, 28 August - 1 September, 2012

Localization and Detection of Breast Cancer Tumors with Digital Image Elasto-Tomography

Elijah E.W. Van Houten, Helen Kershaw, Thomas Lotz, and J. Geoffrey Chase

Abstract— **Digital Image Elasto-Tomography (DIET) is a novel elastic contrast based breast imaging method using time-harmonic motion data obtained from a calibrated array of high resolution digital cameras scanning the tissue surface. The method is currently undergoing initial clinical testing and preliminary results in cases of malignant breast tumors are now available. The method has proved capable of detecting and localizing the stiff lesions within the heterogeneous tissue structure of the beast through the use of an evolution based optimization algorithm implemented in linear finite elements. The method has also proved successful at detecting both inclusion and non-inclusion cases in specially constructed tissue mimicking silicon phantoms.**

I. Introduction

Breast cancer detection and diagnosis has been a longstanding objective for elastographic imaging modalities, including Ultrasound Elastography (UE) [1] [2] and Magnetic Resonance Elastography (MRE) [3] [4] [5], and the high elastic contrast between healthy and malignant tissues these methods seek to exploit has been carefully studied in *ex-vivo* experiments [6]. Digital Image Elasto-Tomography (DIET) was developed in an effort to capitalize on rapid improvements in digital imaging technology as a way of mitigating cost in elastographic imaging systems for breast cancer screening. The method is based on data obtained from a synchronized and calibrated digital camera array able to capture the steady-state motion pattern on the breast surface as it undergoes time harmonic vibration [7]. This information is then processed by a sophisticated image reconstruction algorithm based on genetically encoded optimization implemented in linear elastic finite elements [8]. The result is an estimate of the location and size of any significantly stiff lesions found within the breast, which could be used for further diagnostic evaluation. Some validation work has already been completed for the DIET method using homogeneous and heterogeneous silicon phantoms [9]. Further work has now been completed in specially fabricated homogeneous and heterogeneous tissue mimicking breast phantoms, which shows the method is capable of distinguishing stiff lesions within a heterogeneous background as well as differentiating cases with no significantly stiff inclusions.

This work was supported by a Postdoctoral Fellowship grant (UOCX0807) from the NZ Foundation forResearch, Science and Technology (FRST).

E.E.W. Van Houten is with the Département de génie mécanique, Université de Sherbrooke, Sherbrooke, QC J1K 2R1, Canada (phone: 819 821-8000 x 62153; fax: 819 821-7163; e-mail: eew.vanhouten@usherbrooke.ca).

H. Kershaw, T. Lotz and Prof. J.G. Chase are with the Department of Mechanical Engineering, University of Canterbury, Christchurch, 8041, New Zealand (e-mail: helehkersh@gmail.com; thomas.lotz@canterbury.ac.nz; geoff.chase@canterbury.ac.nz).

II. Methods

A. Motion Imaging

DIET motion data was captured using a prototype clinical imaging system consisting of 5 digital camera units calibrated for 3D registration and synchronized through stroboscopic illumination [10] as shown in Figure 1.

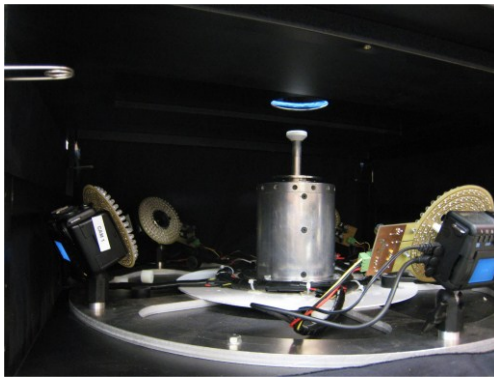

Figure 1: An Early DIET Prototype showing the camera arrangement, the vertical actuator and the ring flash illumination system.

Motion data was captured from the breast surface by tracking a distribution of hundreds of fiducial markers (made of colored paper) applied to the breast surface before the examination [11]. The amplitude and phase of the elliptical motion path for each fiducial are computed based on the trace of the fiducial position through several points along the steady-state, time harmonic vibration. An example of the resulting elliptical motion paths of fiducial markers across the breast surface for one imaging case is shown in Figure 2.

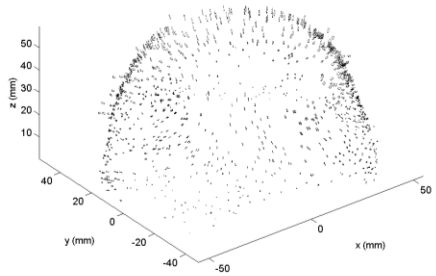

Figure 2: Fiducial motion paths at the breast surface.

B. Inclusion Localization

The localization and size estimation of stiff lesions within the breast is achieved through minimization of a motion based objective function, Φ, measuring the error between the measured displacement field about the breast surface, u^M, and

a set of displacements calculated by linear elastic finite element methods, u^C,

$$\Phi = \tfrac{1}{2}\| u^C - u^M \|^2. \quad (1)$$

In other elastography methods, such as UE and MRE, it is possible to determine an elastic property distribution throughout the tissue volume, $E(x)$, through the solution of

$$E(x) = \arg\min \Phi, \quad (2)$$

through either direct or iterative reconstruction methods [12] [13] [14] [15].

For the DIET method, the lack of displacement data from the breast interior renders the solution of (2) for an arbitrary distribution $E(x)$ highly ill-conditioned. Instead, a *contradictive* reconstruction approach is used, based on a shape based property distribution, where Young's modulus values of either E_I or E_B are assigned based on whether a point x lies within an inclusion or within the background, respectively [9]. The goal of the optimization problem is thus to determine the location and region of the inclusion, which can be defined using simplistic geometry such as a sphere or ellipsoid. The contradictive reconstruction approach involves assuming that a significantly stiff lesion exists within the tissue and allowing the optimization algorithm to contradict this assumption by placing the location of the inclusion outside the tissue volume, thus generating the case where all points x within the tissue are of stiffness E_B. For the DIET method, the stiffness value E_B is considered to be the homogeneous distribution providing the *best-fit* to the measured data according to (1). The inclusion stiffness can either be considered an additional unknown in the localization process or be set at a fixed contrast to the background modulus, e.g. $E_I = 10 \times E_B$.

Even with the improved conditioning of the DIET inverse problem by use of this shape based contradictive approach, the solution of (2) for the most likely property distribution is still not a robust method for the inclusion localization problem, and instead a selection of plausible distributions, $E_i(x)$, is made based on their probability, p, with

$$p_i = \Pi(2\pi\sigma^2)^{-1/2}\exp(-1/2\sigma^2(u^C(E_i) - u^M)^2) \quad (3)$$

for measurement variance, σ. The final elastic property distribution of the DIET method, $E'(x)$, is then calculated by averaging the elastic modulus value at each point based on the predictions of all the plausible distributions, such that

$$E'(x) = (1/M)\Sigma E_i(x) \quad (4)$$

for M plausible distributions. The size of the lesion can then be estimated by the volume of this final distribution having stiffness significantly higher than E_B.

C. Evolutionary Optimization

The limitation of (1) to only include measured displacements at the surface of the breast leads to the introduction of multiple local minima to the objective function, Φ, which can be thought of as a function of all plausible elasticity distributions, $\Phi(E)$. Gradient descent based minimization of Φ is thus not viable from an arbitrary initial estimate for the property distribution, $E_0(x)$, as there is no guarantee that the global minimum of Φ will be found. To avoid this pitfall, a genetic algorithm is implemented to search for suitable distributions, $E_i(x)$, minimizing $\Phi(E)$ and thus possessing a significant likelihood, p_i, of being the true elastic property distribution within the tissue. The genetic algorithm is implemented by encoding the shape based material property description for a *population* of N distributions, $E^j(x)$ (x), j = 1,2,3,…,N, which are gradually modified through *mating* and *mutation* processes through repeating generations, with *natural selection* enforced on the population based on a *fitness*, F^j, evaluated for each member of the population through the use of (1), such that

$$F^j = \Phi(E^j). \quad (5)$$

This process continues until a significant portion of the population evolves to have an identical distribution, in the case of a convergent solution, or until a certain number of generations have passed without convergence. The starting point for the genetic algorithm is a population of distributions each containing a single inclusion at a randomly distributed location within the breast.

D. Multi-Frequency Imaging

To further improve the conditioning of the inverse problem for inclusion localization in DIET, multiple data sets are obtained across a range of frequencies, k, for each imaging case. For the optimization process, a unique background stiffness, $E_{B,k}$, is determined for each frequency and the overall motion error for the imaging case is calculated by combining the objective functions for each individual frequency $\Phi_k = \Phi(E_k)$, normalized by a relative measurement variance which accounts for differences between motion amplitudes and measurement accuracies between the different frequencies.

III. Results

Presented here are a variety of results from the DIET method, achieved both in *in-vivo* clinical experiments and *in-vitro* phantom experiments using specialized, tissue-mimicking silicon phantoms.

TABLE I. PHANTOM RESULTS

Phantom	Lesion Localization Results	
	Volume Fraction [%]	*Centroid Distance [mm]*
P_5	183	19
P_{10}	22	12

A. Phantom Results

To help validate the capability of the DIET method to detect and localize lesions of known location and size, a series of specialized silicon phantoms were constructed, including a homogeneous *healthy* example, P_0, and two *tumor* cases, P_5 and P_{10}, with stiff inclusions of 5 *mm* and 10 *mm* radius, respectively. Data was taken at a range of frequencies from 10 – 40 *Hz*. Results from the two tumor cases are given in Table 1, where the *volume fraction* reports the relative volume of the localized lesion as a percentage of the volume of the actual inclusion while the *centroid distance* indicates the absolute distance between the centroid of the localized lesion and that of the actual inclusion. The shape based reconstruction model in these cases was defined as a spherical inclusion of radius 5 *mm* with $E_I = 30$ *kPa*.

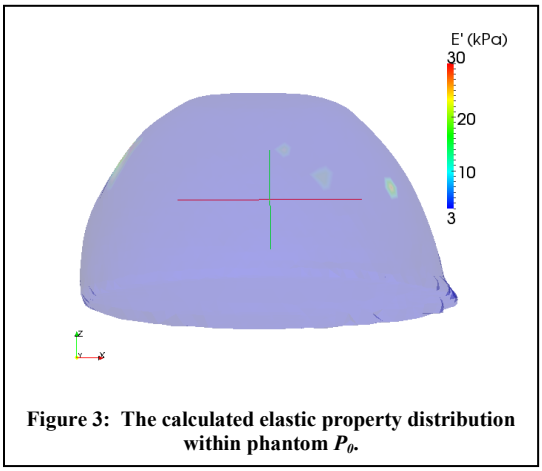

Figure 3: The calculated elastic property distribution within phantom P_0.

Figures 3 – 5 give a graphical representation of the lesion localization results for the 3 phantoms, showing the final elastic property distribution calculated by the DIET method

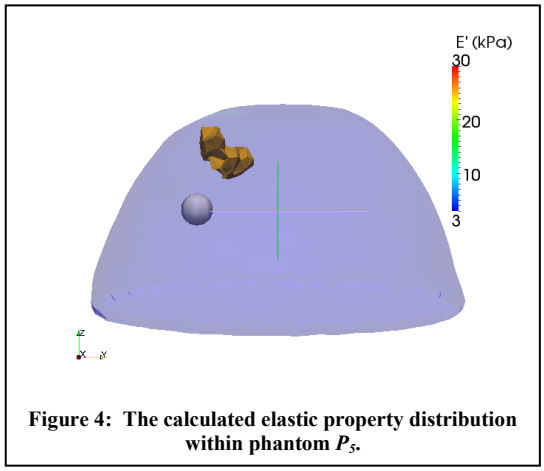

Figure 4: The calculated elastic property distribution within phantom P_5.

via (4). For phantoms P_5 and P_{10}, the actual inclusion size and location is indicated by a white sphere. The effectiveness of the contradictive reconstruction approach is demonstrated in Figure 3, where no region with significant elastic contrast is found to have a high probability of existing within the imaging volume.

B. *In-Vivo Results*

Three cases of cancerous tumors, *C1*, *C2* and *C3*, were imaged with the DIET system. The tumors were detected and classified through traditional mammographic and ultrasound methods, with their approximate location and size recorded in Table 2. Lesion localization was performed for each case using a range of frequencies between 15 – 50 *Hz*. Again, the shape based reconstruction model in these cases was a spherical inclusion of radius 5 *mm* with $E_I = 30$ *kPa*.

TABLE II. *IN-VIVO* CASE DATA

Case	Tumor description based on mammography and ultrasound evaluation	
	Radius [mm]	***Location [hr:min]***
C1	5.5	10:30
C2	15	1:30
C3	17.5	3:00

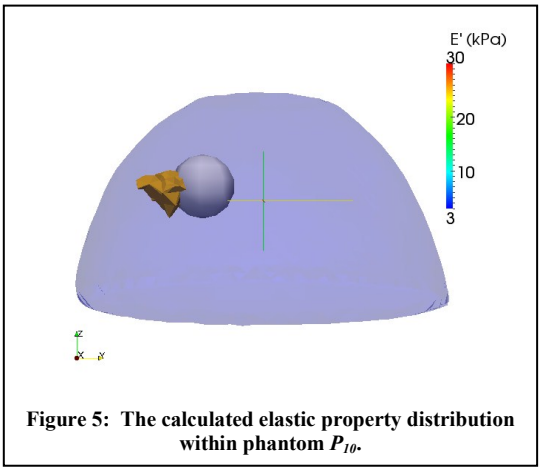

Figure 5: The calculated elastic property distribution within phantom P_{10}.

Table 3 reports the results from the three tumor cases, where the centroid distance information could not be calculated as the exact tumor position, in the geometry of the DIET imaging system, was unknown.

TABLE III. *IN-VIVO* RESULTS

Case	Lesion Localization Results
	Volume Fraction [%]
C1	112
C2	8
C3	54

Figures 6 – 8 give a graphical representation of the lesion localization results for the 3 *in-vivo* tumor cases.

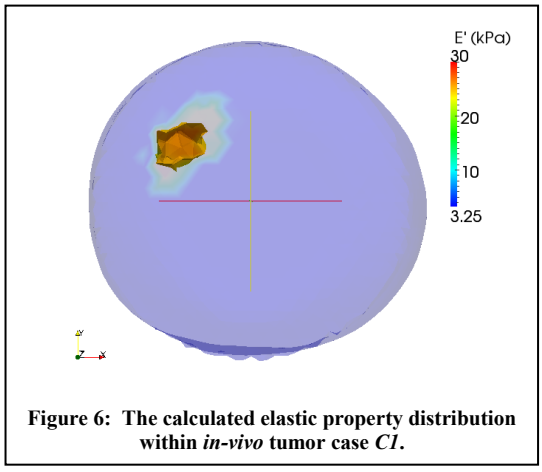

Figure 6: The calculated elastic property distribution within *in-vivo* tumor case *C1*.

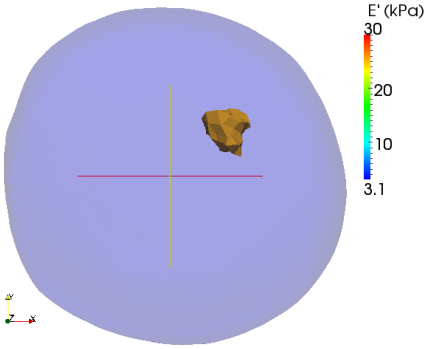

Figure 7: The calculated elastic property distribution within *in-vivo* tumor case *C2*.

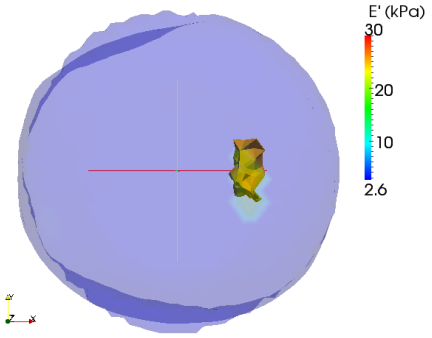

Figure 8: The calculated elastic property distribution within *in-vivo* tumor case *C3*.

IV. Conclusion

In general, the DIET lesion localization problem was capable of correctly identifying the location of high contrast stiff regions within both phantom and *in-vivo* breast tumor cases. Using the contradictive reconstruction approach, the method was also able to distinguish the *healthy* case from the two inclusion cases in the silicon phantom experiments. The accuracy of the size estimation of the various lesions in both phantom and *in-vivo* cases varied, and was somewhat dependant on the agreement between the actual size of the lesion and that used in the shape based reconstruction process. Overall, the method shows promise in the application to breast cancer lesion localization and detection, although certainly much work in development and validation remains to be done.

Acknowledgment

The authors would like to thank the nurses and volunteers at Canterbury Breastcare, Christchurch, NZ, for their contributions in clinical trials of the DIET system.

Elijah E. W. Van Houten is a member of the FRSQ funded *Centre de recherche clinique Étienne-Le Bel.*

References

[1] J. Ophir, I. Cespedes, H. Ponnekanti, Y. Yasdi and X. Li, "Elastography: a quantitative method for imaging the elasticity of biological tissues," *Ultrasonic imaging,* vol. 13, no. 2, pp. 111-134, 1991.

[2] B. Garra, E. Cespedes, J. Ophir, S. Spratt, R. Zuurbier, C. Magnant and M. Pennanen, "Elastography of breast lesions: initial clinical results," *Radiology,* vol. 202, no. 1, pp. 79-86, 1997.

[3] R. Sinkus, J. Lorenzen, D. Schrader, M. Lorenzen, M. Dargatz and D. Holz, "High-resolution tensor mr elastography for breast tumour detection," *Physics in Medicine and Biology,* vol. 45, no. 6, p. 1649, 2000.

[4] E. E. Van Houten, M. Doyley, F. Kennedy, J. Weaver and K. Paulsen, "Initial in vivo experience with steady-state subzone-based MR elastography of the human breast," *Journal of Magnetic Resonance Imaging,* vol. 17, no. 1, pp. 72-85, 2003.

[5] A. Manduca, T. Oliphant, M. Dresner, J. Mahowald, S. Kruse, E. Amromin, J. Felmlee, J. Greenleaf and R. Ehman, "Magnetic resonance elastography: Non-invasive mapping of tissue elasticity," *Medical Image Analysis,* vol. 5, no. 4, pp. 237 - 254, 2001.

[6] A. Samani, J. Zubovits and D. Plewes, "Elastic moduli of normal and pathological human breast tissues: an inversion-technique-based investigation of 169 samples," *Physics in Medicine and Biology,* vol. 52, no. 6, p. 1565, 2007.

[7] T. Lotz, P. Simpson, D. Stocker, C. Hann and J. Chase, "In vitro evaluation of surface based non-invasive breast cancer screening with digital image based elasto tomography (DIET)," in *Engineering in Medicine and Biology Society (EMBC)*, Buenos-Aires, 2010.

[8] A. Peters, J.G.Chase and E. Van Houten, "Digital Image Elasto-Tomography: Combinatorial and Hybrid Optimazation Algorithms for Shape-Based Elastic Property Reconstruction," *IEEE Trans. Biomed. Eng.,* vol. 55, no. 11, pp. 2575-2583, 2008.

[9] A. Peters, J. Chase and E. Van Houten, "Estimating elasticity in heterogeneous phantoms using Digital Image Elasto-Tomography," *Med. Bio. Eng. Comput.,* vol. 47, no. 1, pp. 67-76, 2009.

[10] A. Peters, J.G.Chase and E. Van Houten, "Digital Image Elasto-Tomography: Mechanical Property Estimation Of Silicone Phantoms," *Med. Bio. Eng. Comput.,* vol. 46, no. 3, pp. 205-212, 2008.

[11] R. Brown, C. Hann and J. Chase, "Vision-based 3d surface motion capture for the diet breast cancer screening system," *International Journal of Computer Applications in Technology,* vol. 39, no. 1, p. 72–78, 2010.

[12] P. Barbone and N. Gokhale, "Elastic modulus imaging: on the uniqueness and nonuniqueness of the elastography inverse problem in two dimensions," *Inverse Problems,* vol. 20, no. 1, p. 283, 2004.

[13] R. Sinkus, M. Tanter, S. Catheline, J. Lorenzen, C. Kuhl, E. Sondermann and M. Fink, "Imaging anisotropic and viscous properties of breast tissue by magnetic resonance elastography," *Magnetic Resonance in Medicine,* vol. 53, no. 2, pp. 372-387, 2005.

[14] E. E. Van Houten, A. Peters and J. Chase, "Phantom elasticity reconstruction with Digital Image Elasto-Tomography," *J. Mech. Behav. Biomed. Mtrls.,* vol. 4, no. 8, pp. 1741-1754, 2011.

[15] S. Kruse, J. Smith, A. Lawrence, M. Dresner, A. Manduca, J. Greenleaf and R. Ehman, "Tissue characterization using magnetic resonance elastography: preliminary results," *Physics in Medicine and Biology,* vol. 45, no. 6, p. 1579, 2000.